SSRG International Journal of Electrical and Electronics Engineering
ISSN: 2348-8379/ https://doi.org/10.14445/23488379/IJEEE-V11I5P104

Volume 11 Issue 5, 27-44, May 2024

Original Article

A Novel DG Integrated MF-AUPQC Device for Active-Power Quality Regulation in Utility-Grid Powered EV Charging Stations

Anil Kumar Dharavatu[1], Srinu Naik Ramavathu[2]

[1,2]*Department of Electrical Engineering, Andhra University College of Engineering, Andhra University, Andhra Pradesh, India.*

[1]*Corresponding Author : dharavatuanilkumar.eee@gmail.com*

Received: 03 March 2024 Revised: 04 April 2024 Accepted: 02 May 2024 Published: 29 May 2024

Abstract *- Nowadays, global warming together environmental issues are declining rapidly due to the adoption of Electric Vehicles (EVs) over fossil-fuel-operated Internal Combustion Engine (ICE) vehicles. The substantial replacement of these EVs in the automobile sector has led to decreasing the ecological emissions, vehicle maintenance and running costs. Mostly, EVs are driven by battery packs and charge these batteries through utility-grid integrated charging stations. It is noted that identifying such charging stations may impact the utility grid due to grid-islanding, Power-Quality (PQ) issues, power shortages and, scheduled load interruptions, so on. To overcome the problems above, the modern power generation corridor has been integrated into the utility grid by employing a solar-photovoltaic powered Distributed Generation (DG) scheme. In this regard, mitigation of various PQ issues and integration of solar-PV enabled DG into utility-grid/EV charging stations has been considered as the major problem statement. The main goal of this work is to enhance PQ issues and continuous active-power exchanging support to both EV charging stations and utility-grid levels by proposing a Multi-Functional Active Universal Power-Quality Conditioner (MF-AUPQC) device. The proposed MF-AUPQC device is impressively constituted in both DG and PQ mitigation modes by using a novel Generalized Voltage-Current Reference (GVCR) controller; it extracts the fundamental reference voltage-current signals. The main emphasis of this work is the designing, operation and performance of the proposed GVCR-controlled MF-AUPQC device has been investigated under both DG and PQ mitigation modes by using Matlab/Simulink computing tools, presenting the analysis and interpretation of simulation results.*

Keywords *- Distributed Generation, Electric vehicles charging stations, Generalized Voltage-Current Reference (GVCR) controller, Multi-Functional Active Universal Power-Quality Conditioner, Power-quality regulation.*

1. Introduction

Nowadays, the widespread use of EVs is substantially more privileged to the automobile sector for economical, adaptable, and accessible transportation than fossil-operated ICE vehicles [1]. These EVs are the most significant replacements in the automotive industry, resulting in lower fossil fuel consumption, operating costs, environmental CO_2 emissions, and vehicle maintenance, among other benefits. According to the vehicle registration authorities, 45% of EVs in our nation will be owned by December 2023 and also utilised in a variety of ways, including e-auto rickshaws, e-bikes, EV-cars, and EV-buses [2].

Generally, these EVs are powered by DC battery packs that are charged via electric-grid-connected EV charging stations. Because of the fast growth in EV utilization, the need for EV charging stations has increased significantly. Multiple EV charging infrastructures are planned to be installed in both urban and rural places to address the requisite power demand to cater for the significant barrier in both regions. It should be mentioned that the installation of such new charging stations may introduce serious PQ concerns in the electric grid because of non-linear power-electronic conversion devices in EV charging stations [3, 4].

Although, the utility-grid powered EV charging stations encounter crucial technical concerns related to scheduled block-outs, sudden load interruptions, power shortages, grid islanding, etc. To overcome the above problems, the modern and advanced power generation corridor has been included in to utility-grid by employing a renewable energy-powered Distributed Generation (DG) scheme [5-8]. In this realm, it acts as an energy back-up for delivering continuous power support to EV charging stations and/or utility-grid with respect to required power demand during power shortages and grid-islanding operations.

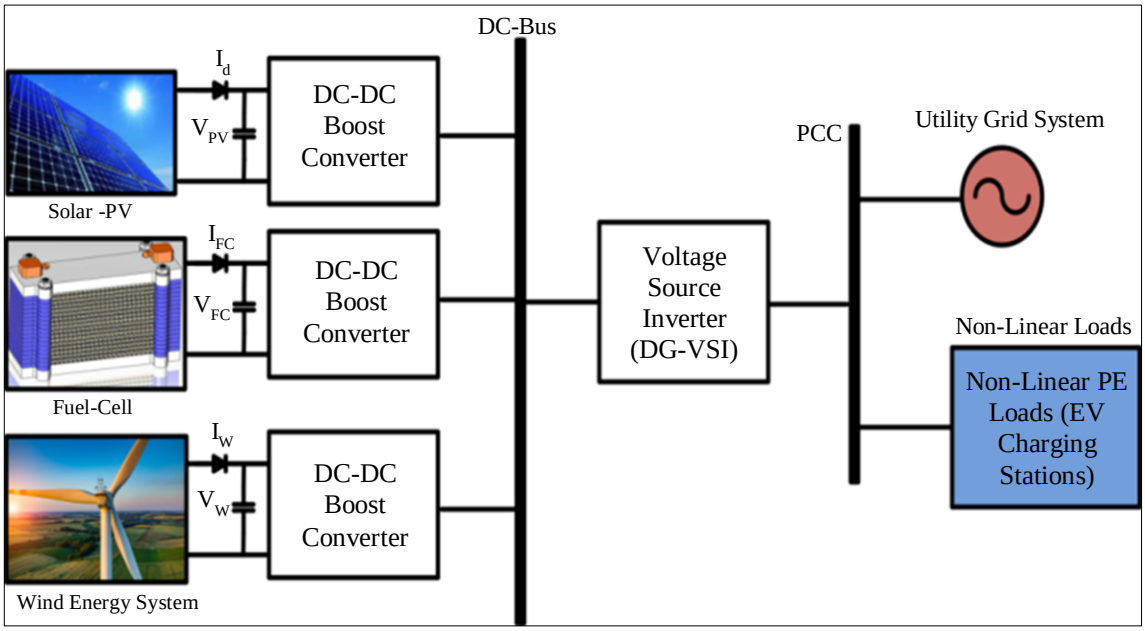

Fig. 1 Schematic model of RES powered DG integration scheme

The contemporary advanced DG scheme is employed for requisite power demand via various Renewable Energy Sources (RES), which offers favorable merits like flexible active-power exchange, no transmission losses/cost and, high power efficiency, maximizing the grid capacity, so on [9, 10].

The schematic model of RES RES-powered DG integration scheme is depicted in Figure 1. Some of the prominent renewable sources like solar-photovoltaic, wind-energy generation biomass, small hydropower plants and, tidal power, so on. Among various renewable energies, the solar-PV is the best selection in most DG integration schemes due to low running cost, virtuous, plentiful nature, high operation life, flexible power, no fuel consumption, etc. In this way, mitigation of various power-quality issues and the integration of accessible solar-PV powered DG into utility-grid/EV charging stations has been considered as the major problem statement [11-13].

The significance of quality power in EV charging stations is enormously recognized due to critical impacts on utility-grid energized distribution networks [14]. The utility grid is proliferated because existence of Non-Linear AC-DC Diode-Bridge Rectifiers (NL-DBRs), which are used for charging the batteries in EV systems through onboard or off-board energy convertible chargers.

The main concern is that the usage of that massive power conversion charger injects harmful harmonic currents into the Common Coupling Point (PCC) of the utility-grid system. These harmful harmonic currents prompt distortions in utility-grid/PCC source current grid frequency as they are causing unbalanced loads, increasing the reactive-power demand, non-unity power-factor and so on. Furthermore, several voltage deviations, such as voltage harmonics and voltage sag-swells, are influencing the performance and operation of multiple EV charging infrastructures in both communities due to power pollution happening in the PCC of utility-grid systems [15, 16].

To address these PQ challenges, many scientists and utility-grid engineers are developing the most advanced PQ mitigation solutions through the Custom-Power Conditioning (CPC) approach [17-22]. Using this CPC approach, several custom-power devices have been created to compensate for related voltage-current PQ difficulties, resulting in a PCC of utility-grid that is fundamental, balanced in nature, and sinusoidal in shape as per IEC/IEEE standards.

The classification of CPC devices has been selected relies on unique PQ issues, such as Active Power Filters (APFs) [23], Distributed Static Compensators (DSTATCOMs) [24], Static Voltage Regulators (SVRs), Dynamic Voltage Regulators (DVRs) [25], and Active Universal Power-Quality Conditioners (AUPQC), among others. Among the CPC mentioned above devices, the AUPQCs have been specially developed for power distribution systems, as discussed in the previous study. The AUPQC has the capability of mitigating any voltage and current PQ concerns on the utility-grid, as well as reactive power exchange with regard to demand, ensuring the quality of power in utility-grid energized EV charging stations.

The AUPQC device structure is emphasized in the previous study, which makes use of two identical Voltage-Source Inverters (VSIs) are consecutively organized as back-

to-back topologies. These two VSIs are configured in a shunt-series manner and connected to the PCC of the utility-grid by means of a common DC source.

The primary goal of the proposed MF-AUPQC device is employed for optimise the various PQ concerns in both utility-grid and the charging station levels and make system specifications as per grid-code standards. Along with PQ enhancement, the MF-AUPQC device acts as DG-VSI; the available solar-PV power is integrated directly into a utility-grid/EV charging station for active power regulation during power shortages and grid-islanding operations.

The proposed DG scheme reduces the cost, size and complex design because no additional DG inverters over the conventional droop-control algorithms are explored in [26, 27]. The primary emphasis of the proposed MF-AUPC device aims to operate in both PQ and DG integration modes for PQ enhancement and active-power regulation in both utility-grid and EV charging stations by adopting a feasible control algorithm.

According to several literature highlights, the most significant reference current and voltage extraction classical control schemes [28] are the Instantaneous Real Power Controller (IRP) [29] and Synchronous Reference Frame Controller (SRF) [30]. The investigation conducted in the above control schemes describes that these schemes suffer several technical limitations, such as intricate mathematical notations, complex frame conversions, high reference signal delay, etc.

However, these complex conversion schemes generate non-fundamental/non-sinusoidal reference current signals with high-level switching frequencies, resulting the high dv/dt switching stress, greater switching losses, and also degrading the overall compensation efficiency, and so on. This is the problem identified in classical SRF/IRP control schemes [29, 30], and these schemes are not suitable for present compensation strategies.

The technical limitations in classical SRF/IRP control schemes are alleviated by proposing the novel Generalized Voltage-Current Reference (GVCR) control scheme. In this work, the proposed MF-AUPQC device is impressively constituted in both DG and PQ mitigation modes by using a novel GVCR controller; it extracts the fundamental reference voltage-current signals for improved compensation characteristics.

The main emphasis of this work is the designing, operation and performance of the proposed GVCR-controlled MF-AUPQC device has been investigated under both DG and PQ mitigation modes by using Matlab/Simulink computing tools, and the analysis and interpretation of simulation results are presented.

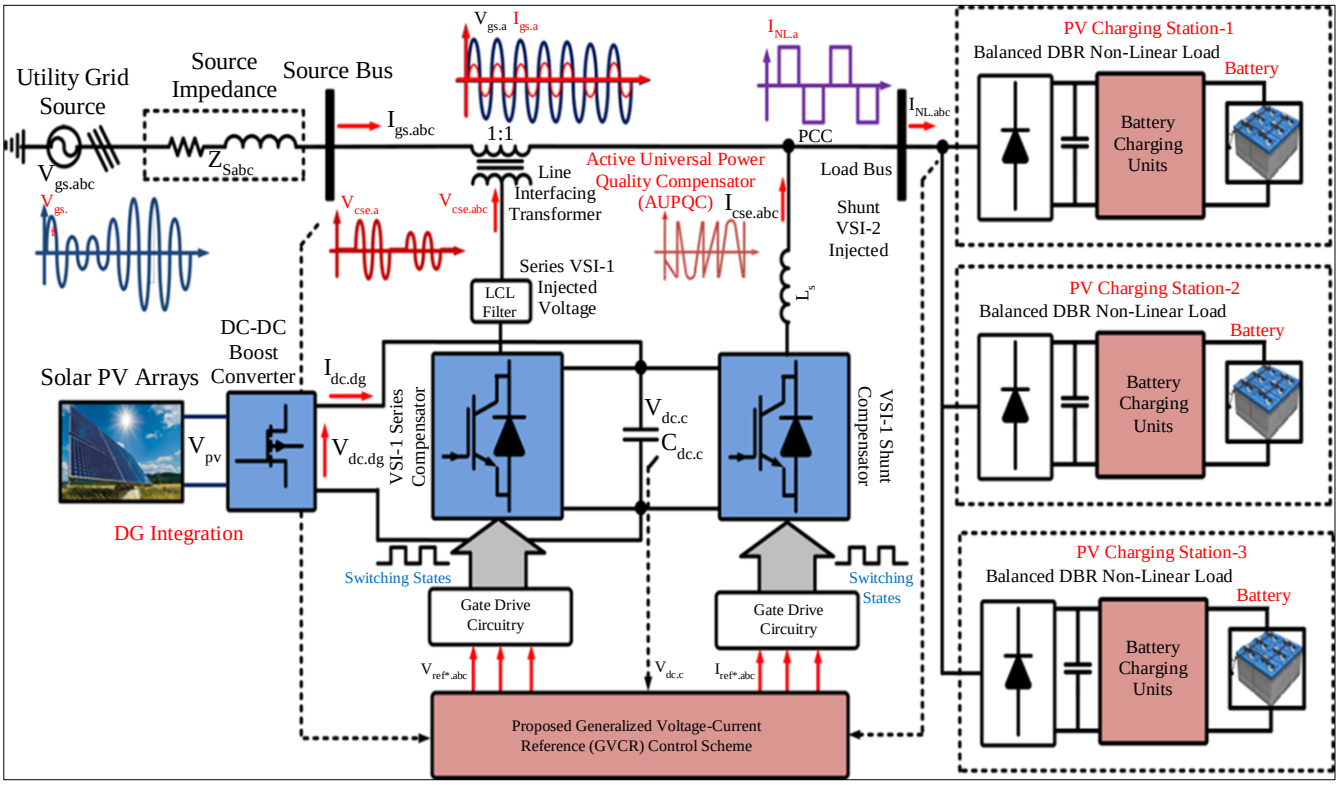

Fig. 2 Schematic model of proposed MF-AUPQC device for both PQ enhancement and DG integration in utility-grid powered EV charging stations

2. Proposed Multi-Functional AUPQC Device for Both PQ and DG Integration in EV Charging Stations

The schematic model of the proposed MF-AUPQC device for both PQ enhancement and DG integration in utility-grid powered EV charging stations is shown in Figure 2. It involves a three-phase utility-grid/PCC source voltage of $V_{gs.abc}$ with grid/PCC source current of $I_{gs.abc}$ delivering through grid/PCC source impedance of $Z_{S.abc}$; these parameters have been used for energizing the non-linear DBR's in EV charging stations with a non-linear load voltage of $V_{NL.abc}$ and current of $I_{NL.abc}$, respectively. In this way, the batteries in EVs are charged through either onboard or off-board EV chargers in charging stations, which are powered by utility-grid system.

These EV chargers consist of massive non-linear DBRs, which convert the available AC utility-grid power into constant DC power with a constant voltage to make batteries as required full state-of-charge through charge control. These non-linear DBRs are placed at the front end of EV chargers for charging the battery packs; they produce harmful harmonic current distortions in the utility-grid/PCC of the distribution network and also affect the other loads.

However, there is another constraint: the non-linear load voltage on the EV charging station side has been affected due to the appearance of voltage harmonics, voltage swells, voltage sags, and so on. The proposed GVCR-controlled MF-AUPQC device represents the multi-functions in utility-grid powered EV charging stations, such as

- Power-quality enhancement in both utility-grid/PCC and the EV charging station levels,
- DG integration for active power regulation during power shortages and grid-islanding operations.

The MF-AUPQC structure comprises dual VSI modules, which are consecutively interfaced to the PCC of the utility-grid as series VSI-1 and shunt VSI-2 energized through common DC-link capacitor $C_{dc.c}$ with a constant voltage of $V_{dc.c}$. The VSI-1 of the MF-AUPQC device is considered a series-active power filter for compensation of voltage-affected PQ issues such as voltage harmonics, voltage sag-swells, and voltage interruptions occurring in utility-grid/PCC level.

When any voltage deviations are influenced in the utility-grid that affects the grid-code limits attained, voltage issues are counteracted by series VSI-1 of MF-AUPQC device. This series VSI-1 functions as an in-phase injection principle which injects the required voltage into PCC to make non-linear load voltage as sinusoidal, balanced, constant and fundamental. During compensation, the unwanted notches produced by series VSI-1 are eliminated by using back-end line filters, which allow varying voltages for continuously regulating the load voltage support to EV chargers in charging stations.

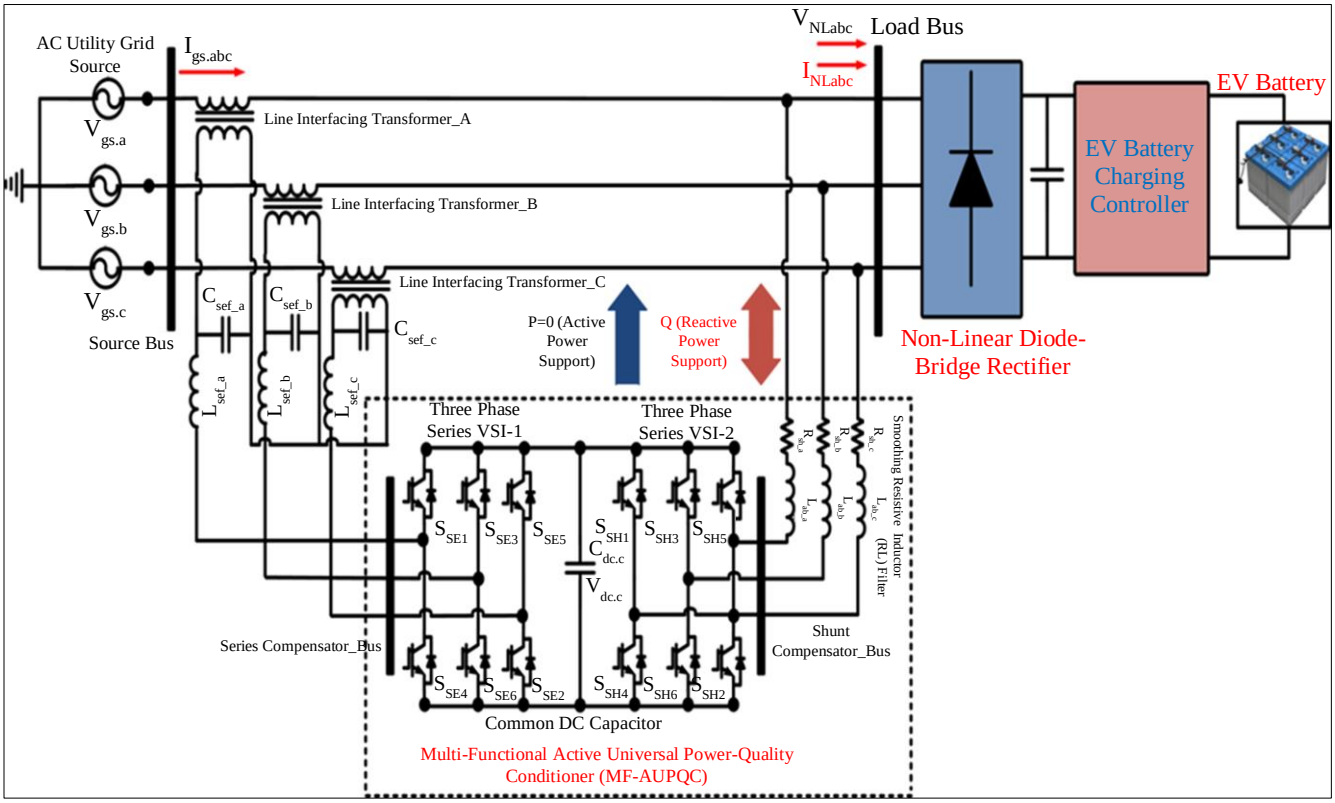

Fig. 3 Block diagram of PQ compensation (without DG) in utility-grid powered EV charging stations

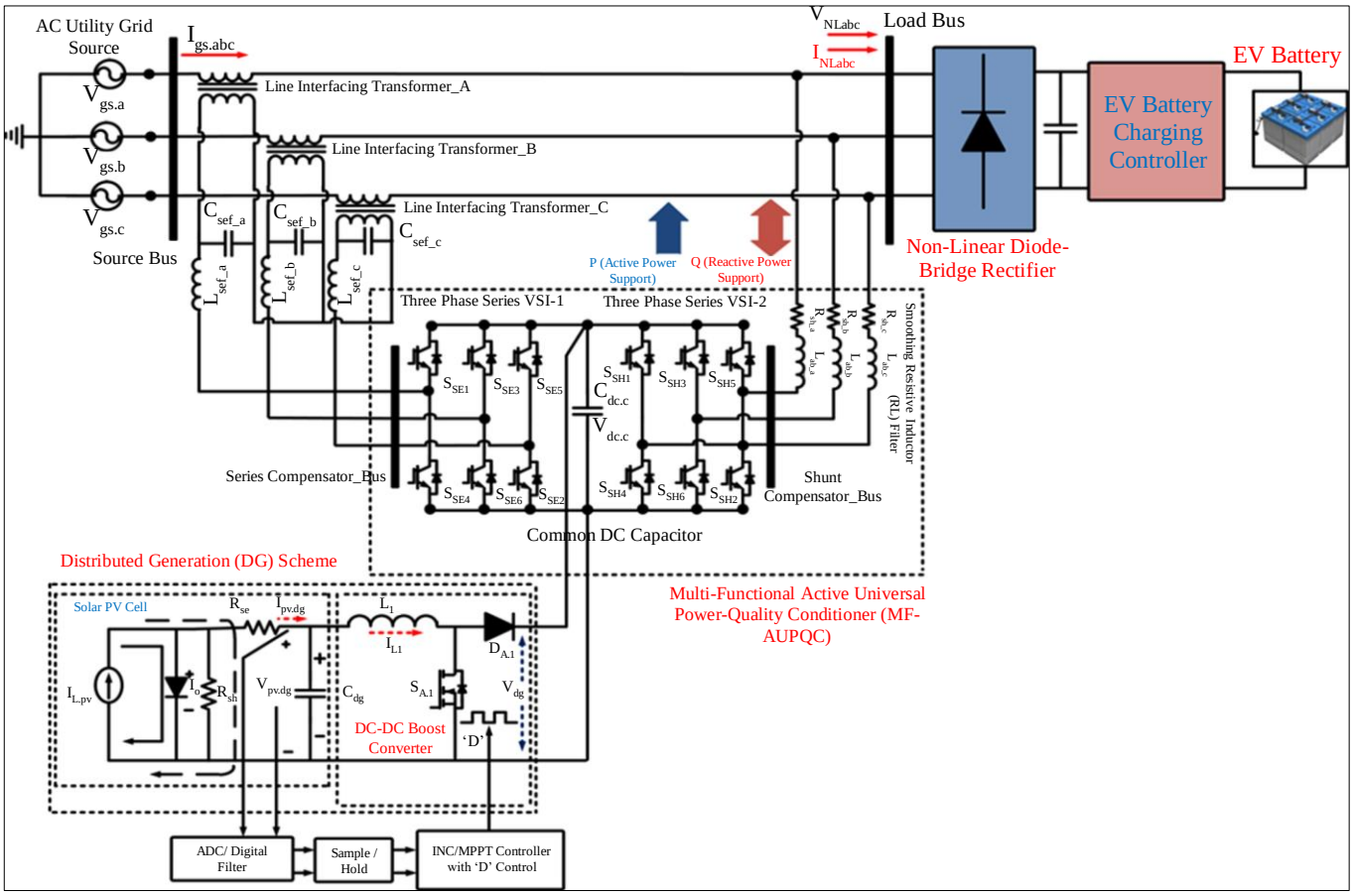

Fig. 4 Block diagram of DG integration scheme (with DG) in utility-grid powered EV charging stations

The VSI-2 of the MF-AUPQC device is considered a shunt-active power filter for compensation of current affected PQ issues such as current harmonics coming, reactive power support, load balance, and power-factor correction occurring from non-linear DBRs of EV charging stations. When any current distortions are influenced in the PCC of the utility-grid that affects the IEEE/IEC standards, and that distorted grid/PCC source current is counteracted by shunt VSI-2 of MF-AUPQC device.

The shunt VSI-2 functioned as an in-phase opposition current injection principle, which injects the requisite current into the grid/PCC to define source currents as balanced, linear, sinusoidal and fundamental. During compensation, the unwanted notches produced by shunt VSI-2 are eliminated by using back-end line filters, which allow varying currents for continuously regulating the reactive power and maintaining the ideal power factor in the grid/PCC of the utility distribution system.

The block diagram of PQ compensation (without DG) in utility-grid powered EV charging stations is illustrated in Figure 3. In recent days, the DG has been one of the significant components of a utility grid system; it is the backbone of modern power distribution systems. It has received wide publicity because of its key merits, such as reliability, maximum efficiency by decreasing transmission loss and cost, enhancing the voltage profile and security, etc.

In this case, solar-PV acts as a major source of DG and the produced solar-PV power has been controlled by using a front-end DC-DC boost converter with an Incremental-Conductance (INC) Maximum-Power Point Tracker (MPPT) algorithm. During available solar-PV power, it reduces the consumption of grid active-power by delivering the required power to energize the non-linear DBRs of EV charging stations with respect to certain load demands.

The operating principle of the DG scheme is manifested based on the current sharing principle between the utility-grid and the solar PV system. The energy management between both sources is evaluated based on sensing the required current and the availability of solar-PV power at when constant irradiance level.

During high irradiance levels, the INC-MPPT-controlled solar PV delivers the maximum current, and the utility-grid delivers the minimum current with respect to the required load current demand. During low irradiance levels, the INC-MPPT-controlled solar PV delivers the minimum current, and

the utility-grid delivers the maximum current with respect to the required load current demand. The main advantage of the DG scheme is, that it avoids the use of additional complex DG-VSI's and its control droop control algorithm.

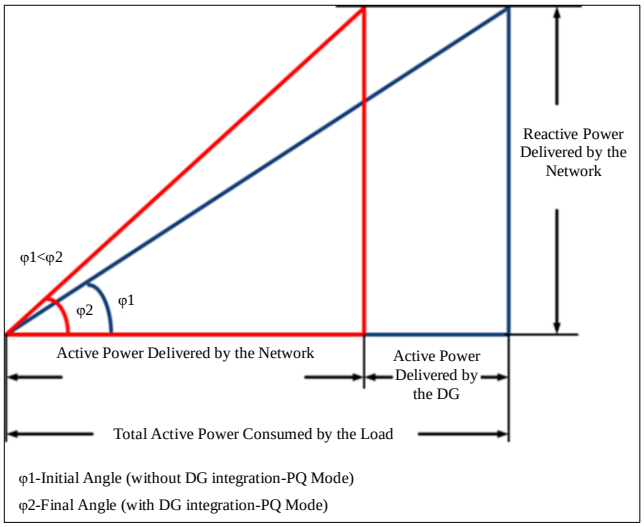

Fig. 5 Graphical representation of the PQ and DG integration modes

The shunt VSI-2 of MF-AUPQC device acts as DG-VSI, which saves size, cost and compact energy generation scheme. The block diagram of the DG integration scheme (with DG) in utility-grid powered EV charging stations is illustrated in Figure 4. Thus, the proposed GVCR-controlled MF-AUPQC device enhances the PQ and active-power support by DG in utility-grid powered EV charging stations adhering to IEC/IEEE standards. The graphical representation of the PQ and DG integration modes is clearly shown in Figure 5.

3. Proposed GVCR Control Algorithm

The operation and performance of the proposed MF-AUPQC device mostly rely on a well-acclaimed proposed GVCR control algorithm for extracting the feasible voltage-current reference signals. This algorithm helps to reduce the crucial problems in classical SRF/IRP control schemes; it can produce fundamental switching frequency-based voltage-current reference signals to both series and shunt VSIs of MF-AUPQC devices.

It is noted that the major advantages of using the proposed GVCR control algorithm are low response latency in reference voltage-current signals, simple mathematical notations, low dv/dt stress, low switching losses and maximizing the overall compensator efficiency. The extracted three-phase utility grid/PCC voltages and currents are represented as,

$$V_{gs.a} = V_{m.a}\ \sin\theta s$$

$$V_{gs.b} = V_{m.b}\ sin\left(\theta s - {}^{2\pi}/_{3}\right)$$

$$V_{gs.c} = V_{m.c}\ sin\left(\theta s + {}^{2\pi}/_{3}\right) \qquad (1)$$

$$i_{gs.a} = \sum I_{ma.n}\ \sin(n(\omega t) - \theta_{a-n})$$

$$i_{gs.b} = \sum I_{mb.n}\ \sin(n\left(\omega t - \frac{2\pi}{3}\right) - \theta_{b-n})$$

$$i_{gs.c} = \sum I_{mc.n}\ \sin(n\left(\omega t + \frac{2\pi}{3}\right) - \theta_{c-n}) \qquad (2)$$

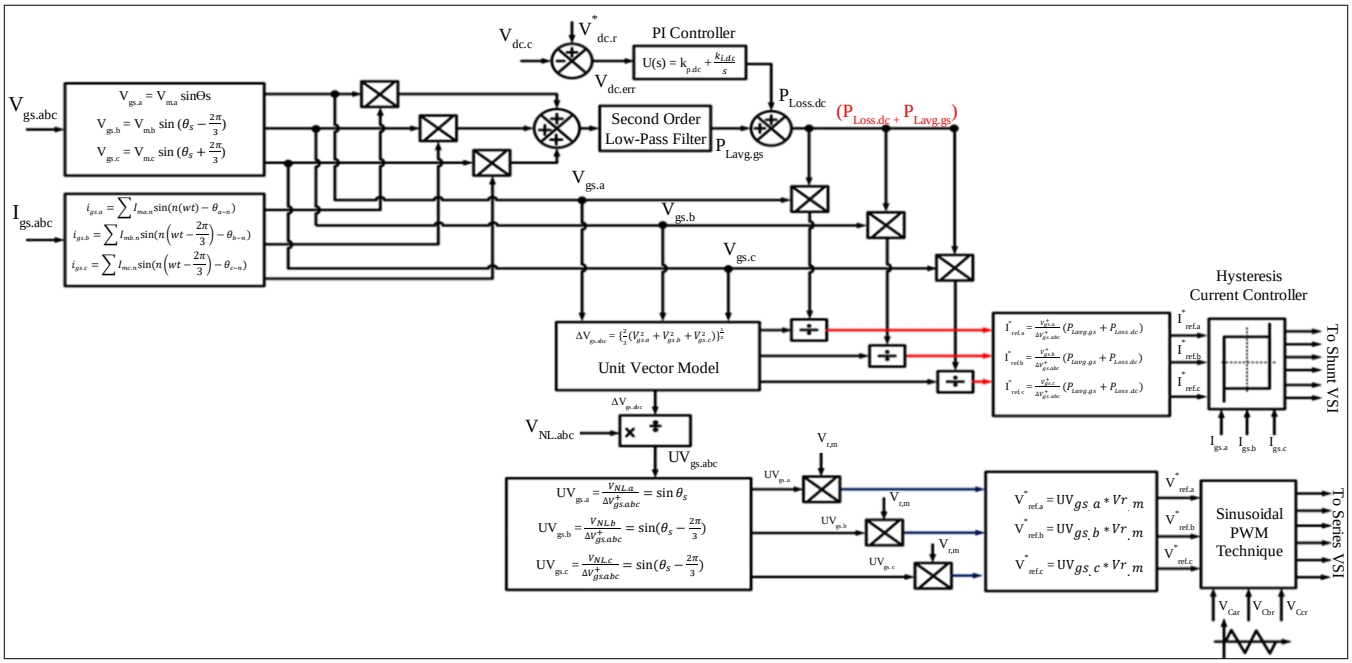

Fig. 6 Schematic diagram of proposed GVCR control algorithm for MF-AUPQC device

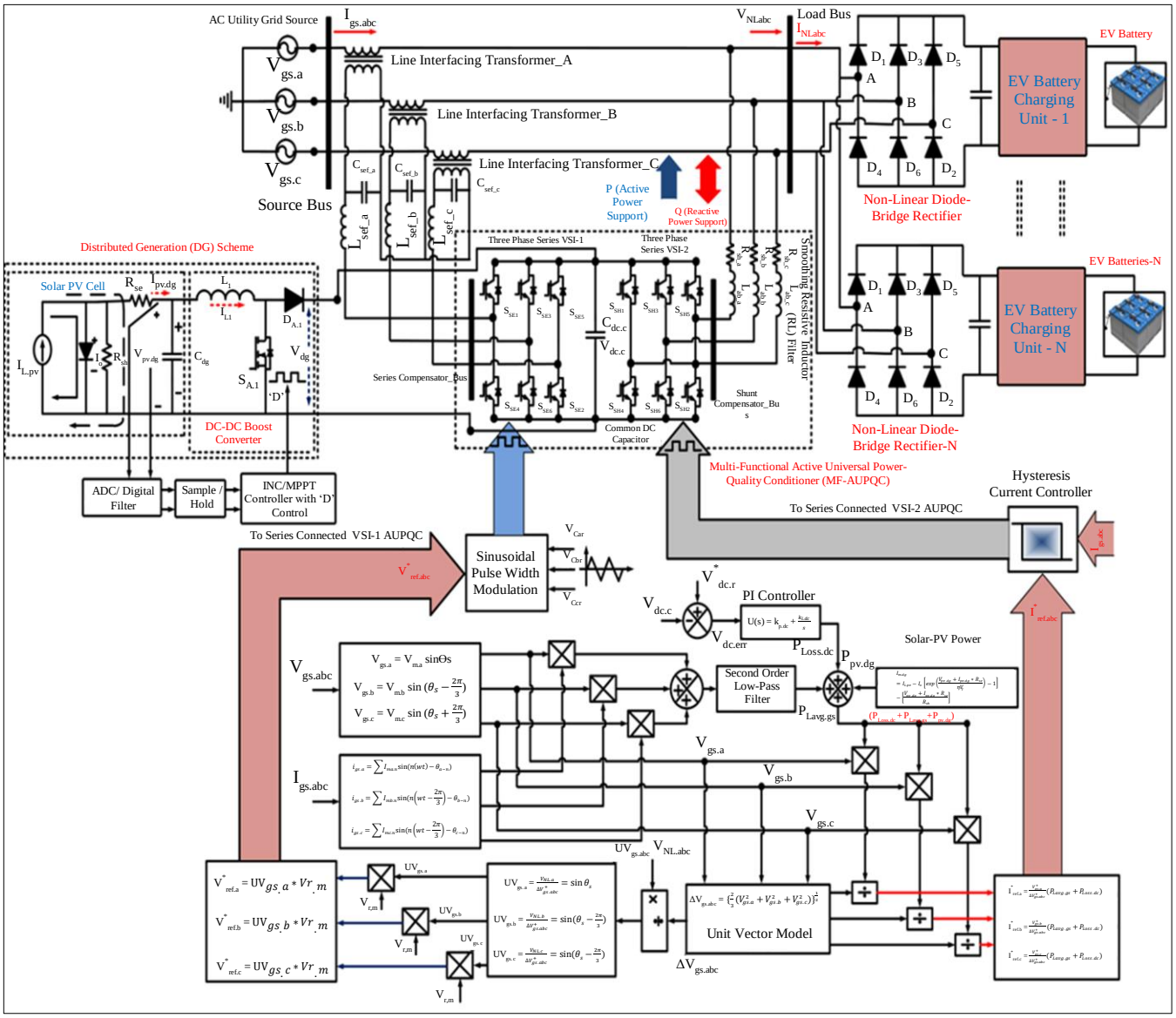

Fig. 7 Overall schematic diagram of novel GVCR controlled MF-AUPQC device for PQ enhancement and DG integration in utility-grid powered EV charging stations

These extracted equivalent three-phase grid/PCC voltages and currents are multiplied and summated each other to attain average grid power ($P_{Lavg.gs}$) in a specified time, instant 't' is represented as below,

$$P_{Lavg.gs} = \frac{1}{T}\int_{t-T}^{T}\left(V_{gs.a}i_{gs.a} + V_{gs.b}i_{gs.b} + V_{gs.c}i_{gs.c}\right)dt \quad (3)$$

The schematic diagram of the proposed GVCR control algorithm for the MF-AUPQC device is depicted in Figure 6. The extracted average grid power (P_(Lavg.gs)) are approximated with a Second-Order Low-Pass Filter (SO-LPF) to allow a lower-order sequence which produces the definite fundamental frequency based reference current signals. Another side, the loss component (P_(Loss.dc)) is attained by comparing the actual (V_(dc.c)) and reference (V_(dc.r)^*) DC-link voltage of DC-link capacitor.

Then, it produces error signals (V_(dc.err)), which are eliminated by using Proportional-Integral (PI) controller with proper proportional (K_(p.dc)) and integral (K_(i.dc)) gain values. It reduces the circulation current flow between the series VSI-1 and shunt VSI-2 of the MF-AUPQC device and helps to maintain DC-link voltage as constant. Thus, ($P_{Loss.dc}$) is represented as,

$$V_{dc.err} = V^{*}_{dc.r} - V_{dc.c} \quad (4)$$

$$P_{Loss.dc} = K_{p.dc}(V_{dc.err}) + K_{i.dc}\int(V_{dc.err})dt \quad (5)$$

The extracted solar-PV power from solar-PV voltage and current under DG integration mode is represented as,

$$I_{m.dg} = I_{L.pv} - I_o\left[exp\left(\frac{V_{pv.dg} + I_{pv.dg} * R_{se}}{\eta V_T}\right) - 1\right] - \left[\frac{V_{pv.dg} + I_{pv.dg} * R_{se}}{R_{sh}}\right]$$

$$P_{pv.dg} = V_{pv.dg} \times I_{pv.dg} \quad (6)$$

The low-frequency fundamental reference average power ($P_{Lavg.gs}$) and loss component in DC power ($P_{Loss.dc}$) is summated with solar-PV power ($P_{pv.dg}$) for the generation of the actual current signal. Based on the above Equations 3, 5 and 6, the final fundamental reference current ($i^*_{ref.abc}$) in the positive sequence is represented as,

$$i^*_{ref.a} = \frac{V^+_{gs.a}}{\Delta V^+_{gs.abc}}\left(P_{Lavg.gs} + P_{Loss.dc} + P_{pv.dg}\right)$$

$$i^*_{ref.b} = \frac{V^+_{gs.b}}{\Delta V^+_{gs.abc}}\left(P_{Lavg.gs} + P_{Loss.dc} + P_{pv.dg}\right)$$

$$i^*_{ref.c} = \frac{V^+_{gs.c}}{\Delta V^+_{gs.abc}}\left(P_{Lavg.gs} + P_{Loss.dc} + P_{pv.dg}\right) \quad (7)$$

Where, ($\Delta V^+_{gs.abc}$) is the non-complex unit-vector sequence is represented as,

$$\Delta V^+_{gs.abc} = \left\{\frac{2}{3}(V^2_{gs.a} + V^2_{gs.b} + V^2_{gs.c})\right\}^{1/2} \quad (8)$$

The reference voltage signal for series VSI-1 of MF-AUPQC device is extracted through a non-complex unit-vector sequence and is differentiated with actual grid voltage is represented as,

$$UV_{gs.a} = \frac{V_{NL.a}}{\Delta V^+_{gs.abc}} = sin\theta s$$

$$UV_{gs.b} = \frac{V_{NL.b}}{\Delta V^+_{gs.abc}} = sin\left(\theta s - 2\pi/3\right)$$

$$UV_{gs.c} = \frac{V_{NL.c}}{\Delta V^+_{gs.abc}} = sin\left(\theta s + 2\pi/3\right) \quad (9)$$

The extracted unit-vector signal ($UV_{gs.abc}$) is compared with the reference voltage magnitude ($V_{r.m}$), then it delivers the final voltage reference signal (V^*_{refabc}) which is represented as,

$$V^*_{ref.a} = UV_{gs.a} * V_{r.m}$$

$$V^*_{ref.b} = UV_{gs.b} * V_{r.m}$$

$$V^*_{ref.c} = UV_{gs.c} * V_{r.m} \quad (10)$$

Finally, the reference current ($i^*_{ref.abc}$) signal is differentiated from the actual grid current ($i_{gs.abc}$), for the generation of a possible switching scheme to shunt connected VSI-2 of MF-AUPQC device. It compensates for the current associated PQ issues by using Hysteresis Current Controller (HCC) drive circuitry. This HCC driver circuit produces the possible switching pulses to switches of VSI-2 through selected Hysteresis band limits.

These band limits act as saturated values of actual and reference currents, which are rotated in between these lower/upper bands are described as conduction-ON or conduction-OFF states of VSI-2 of MF-AUPQC device. And also, the final reference voltage signal ($V^*_{ref.abc}$) is compared with triangular carrier signals ($V_{Cabc.ref}$) for generation of possible switching pattern to series VSI-1 of MF-AUPQC device for compensation of voltage PQ issues by using Sinusoidal Pulse-Width Modulation (SPWM) gate-drive circuitry. The overall schematic diagram of the novel GVCR-controlled MF-AUPQC device for both PQ and DG operations in utility-grid powered charging stations is shown in Figure 7.

Table 1. System simulink data

S. No.	Simulink Components	Values
1	Utility-Grid/PCC Voltage	$V_{gs.abc}$=415V, F_{gs}=50Hz
2	Utility-Grid/PCC Impedance	R_{gs}=0.1Ω, L_{gs}=0.9mH
3	DBR's Non-Linear Load Impedance (Number of EV Chargers)	Charger 1-$R_{NL.abc}$=5Ω to 25 Ω, $L_{NL.abc}$-30mH Charger 2-$R_{NL.abc}$=15Ω to 25 Ω, $L_{NL.abc}$-30mH Charger 3-$R_{NL.abc}$=25Ω to 25 Ω, $L_{NL.abc}$-30mH
4	DC-link voltage & Capacitor Value	$V_{dc.c}$=880V, $C_{dc.c}$=1500µF
5	Shunt VSI-2 Filter	R_{shf}=0.1Ω, L_{shf}=5mH
6	Series VSI-1 Filter	R_{sef}=1Ω, C_{sef}=150µF
7	PI Gain Values	$K_{p.dc}$=0.5, $K_{i.dc}$=0.15
8	1:1 Line Interface Linear Transformer	$V_{gs.abc}$=415V, $P_{gs.abc}$=5KVA, $X_{gs.abc}$=10% of Leakage Reactance
9	Solar-PV (DG) Specifications	$P_{pv.dg}$=880V, $I_{pv.dg}$= 20A, $P_{pv.dg}$=18KW

4. Results and Discussion

The design and performance of the proposed GVCR controlled MF-AUPQC device have been investigated under both DG and PQ mitigation modes by using Matlab/Simulink computing tool; simulation results are presented and verified with different transitions. The system Simulink data is presented in Table 1.

4.1. Compensation of Harmonic Current Distortions in Utility-Grid/PCC Powered Single EV-Charger by Using Proposed GVCR Controlled Shunt VSI-2 of MF-AUPQC Device

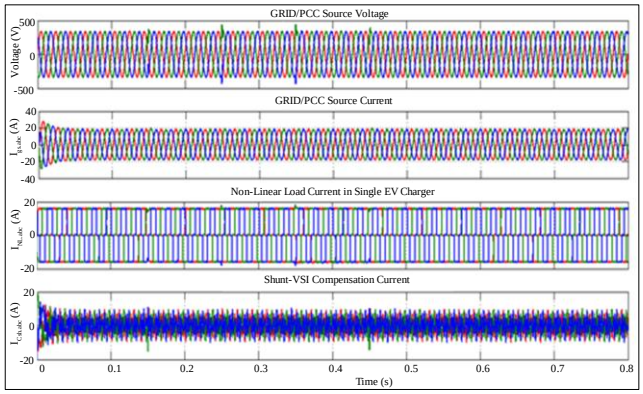

(a) Utility grid/PCC source voltage, (b) Grid/PCC source current, (c) Non-linear load current in single EV charger, and (d) Shunt VSI-2 compensation current

Fig. 8 Simulation results of harmonic current compensation in utility-grid/PCC powered single EV-charger by using proposed GVCR controlled shunt VSI-2 of MF-AUPQC device

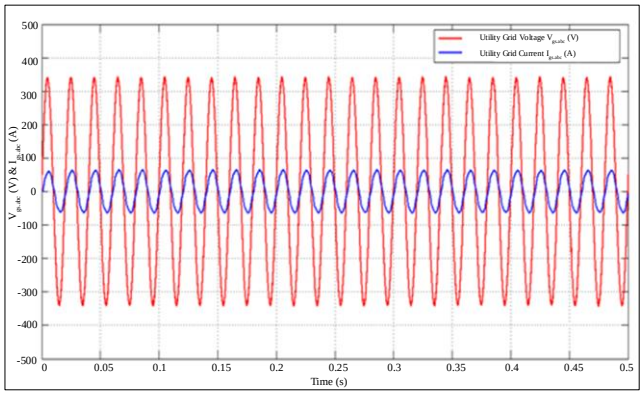

Fig. 9 In-phase of utility-grid/PCC source voltage & current (single EV charger)

The simulation results of harmonic current compensation in utility-grid/PCC powered single EV-charger by using proposed GVCR controlled shunt VSI-2 of MF-AUPQC device are depicted in Figure 8. The single-EV charger comprises of single non-linear DBR is employed which is powered by three-phase distribution network via utility-grid source with a voltage of $V_{gs.abc}$-415V_{rms} and constant system frequency of F_{gs}-50Hz is shown in Figure 8(a). The front-end non-linear DBR module in the charging unit is used for charging the EV batteries through the AC to DC conversion principle. During this conversion principle, the DBR injects the harmful harmonic currents into the PCC of utility-grid system. These harmful harmonic currents prompt the distortions in utility-grid/PCC source current grid frequency as they are causing unbalanced loads, increasing the reactive-power demand, non-unity power-factor and so on.

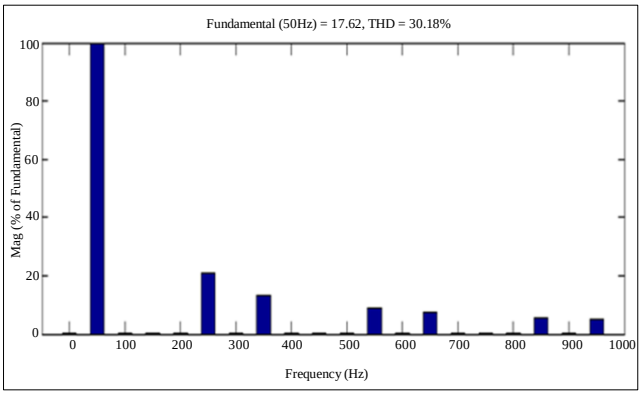

(a) THD spectrum of non-linear load current in single EV charger

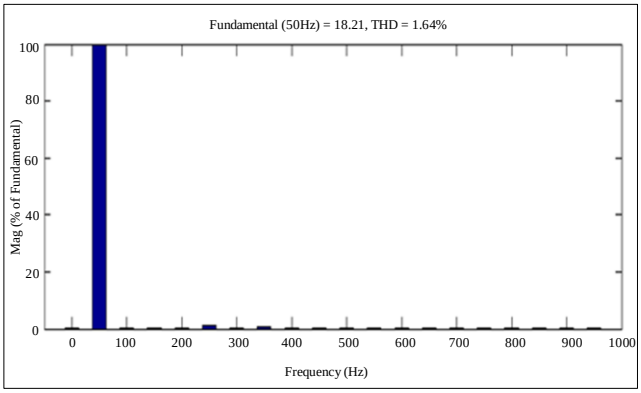

(b) THD spectrum of utility-grid/PCC source current

Fig. 10 THD spectrum analysis during current harmonics compensation (single EV charger)

This DBR module influences the performance and operation of multiple EV charging infrastructures in both communities due to power pollution in the PCC of utility-grid system. For mitigating these issues, the proposed GVCR controlled shunt VSI-2 of MF-AUPQC device has been enabled for mitigation of harmful harmonic current distortions at PCC of utility-grid system.

It functions based on the "in-phase opposition current injection principle", which injects the required compensation current into grid/PCC to make the source current a balanced, linear, sinusoidal and fundamental nature. It maintains the utility-grid/PCC current as a balanced and sinusoidal shape with a value of 18A for delivering the non-linear DBR load current of 16A, as shown in Figure 8 (b), and (c). The shunt VSI-2 injects the requisite compensation current of 8A via line interface filters, as shown in Figure 8(d), respectively. Mainly, the proposed GVCR algorithm enables the extraction of

fundamental reference currents and helps to produce the feasible switching states to shunt VSI-2 of MF-AUPQC device for PQ enhancement as per IEC/IEEE standards.

For this compensation, thus utility-grid/PCC current is served as in-phase with the PCC source voltage to maintain the ideal power factor at the grid/PCC of the distribution network, which is shown in Figure 9. The THD spectrum analysis of the non-linear load current of single-EV charger integration is computed with a value of 30.18%. The THD spectrum analysis of utility-grid/PCC source current is computed with a value of 1.64% is depicted in Figure 10 (a), and (b), which is well-being as per IEEE-519/2022 limits.

4.2. Compensation of Harmonic Current Distortions in Utility-Grid/PCC Powered Dual EV-Chargers by Using Proposed GVCR Controlled Shunt VSI-2 of MF-AUPQC Device

The simulation results of harmonic current compensation in utility-grid/PCC powered dual EV-chargers by using the proposed GVCR controlled shunt VSI-2 of MF-AUPQC device are depicted in Figure 11. The dual-EV chargers comprised of two non-linear DBR is employed which is powered by three-phase distribution network via utility-grid source with a voltage of $V_{gs.abc}$-415V_{rms} and constant system frequency of F_{gs}-50Hz is shown in Figure 11(a).

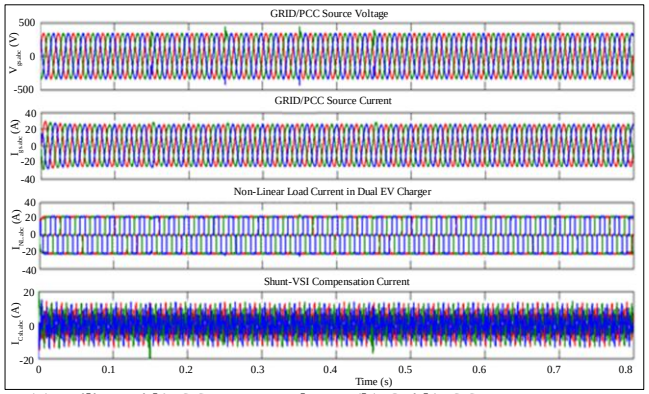

(a) Utility grid/PCC source voltage, (b) Grid/PCC source current, (c) Non-linear load current in dual EV chargers, and (d) Shunt VSI-2 compensation current

Fig. 11 Simulation results of harmonic current compensation in utility-grid/PCC powered dual EV-chargers by using proposed GVCR controlled shunt VSI-2 of MF-AUPQC device

The front-end non-linear DBR modules in the charging unit are used for charging the EV batteries through the AC to DC conversion principle. During this conversion principle, the dual DBR injects massive harmful harmonic currents into the PCC of utility-grid system. These massive harmonic currents prompt the distortions in utility-grid/PCC source current grid frequency as they are causing the unbalanced loads, increasing the reactive-power demand, non-unity power-factor and so on. These DBR modules are highly influencing the performance and operation of multiple EV charging infrastructures in both communities due to power pollution happening in the PCC of utility-grid systems.

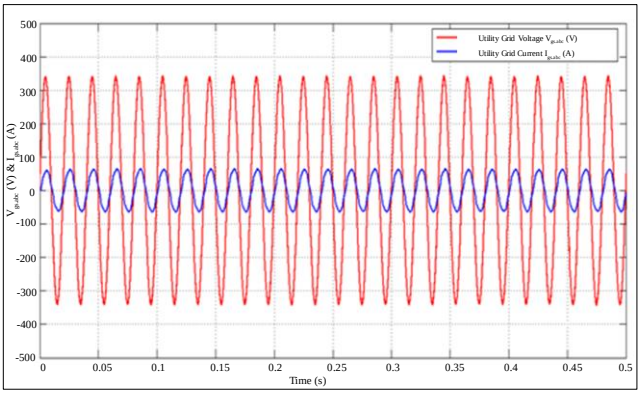

Fig. 12 In-phase of utility-grid/PCC source voltage & current (dual EV charger)

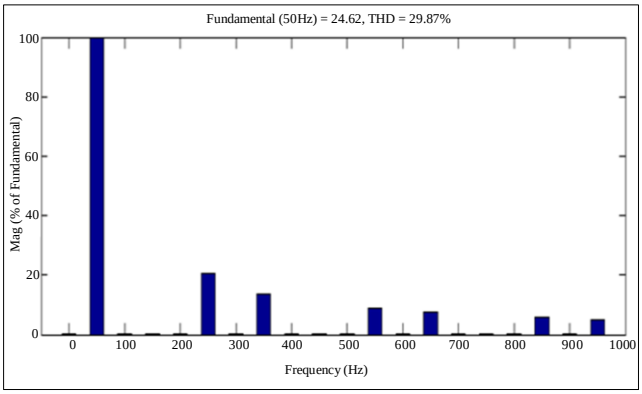

(a) THD spectrum of non-linear load current in dual EV chargers

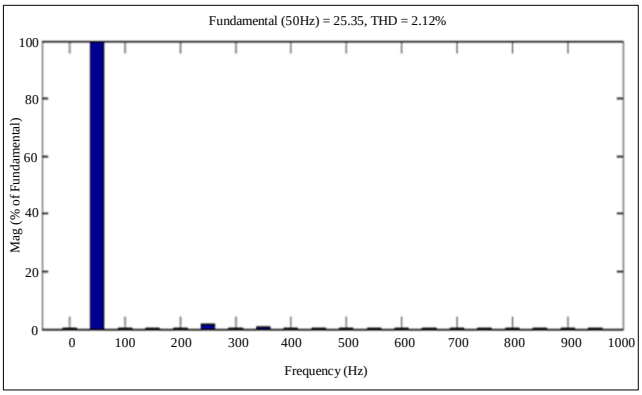

(b) THD spectrum of utility-grid/PCC source current

Fig. 13 THD spectrum analysis during current harmonics compensation (dual EV charger)

For mitigating these issues, the proposed GVCR controlled shunt VSI-2 of MF-AUPQC device has been enabled for mitigation of massive harmonic current distortions at PCC of utility-grid system. It functions based on the "in-phase opposition current injection principle", which injects the required compensation current into grid/PCC to make the source current a balanced, linear, sinusoidal and fundamental nature.

It maintains the utility-grid/PCC current as a balanced and sinusoidal shape with a value of 25A for delivering the non-linear DBR load current of 22A, as shown in Figures 11(b) and 11(c). The shunt VSI-2 injects the requisite compensation current of 13.5 A via line interface filters, as shown in Figure 11(d), respectively. Mainly, the proposed GVCR algorithm enables the extraction of fundamental reference currents and helps to produce the feasible switching states to shunt VSI-2 of MF-AUPQC device for PQ enhancement as per IEC/IEEE standards.

For this compensation, thus utility-grid/PCC current is served as in-phase with the PCC source voltage to maintain the ideal power factor at the grid/PCC of the distribution network, which is shown in Figure 12. The THD spectrum analysis of the non-linear load current of dual-EV chargers integration is computed with a value of 29.87%. The THD spectrum analysis of utility-grid/PCC source current is computed with a value of 2.12% is depicted in Figures 13(a), and 13(b), which is well-being as per IEEE-519/2022 limits.

4.3. Compensation of Harmonic Current Distortions in Utility-Grid/PCC Powered Triple EV-Chargers by Using Proposed GVCR Controlled Shunt VSI-2 of MF-AUPQC Device

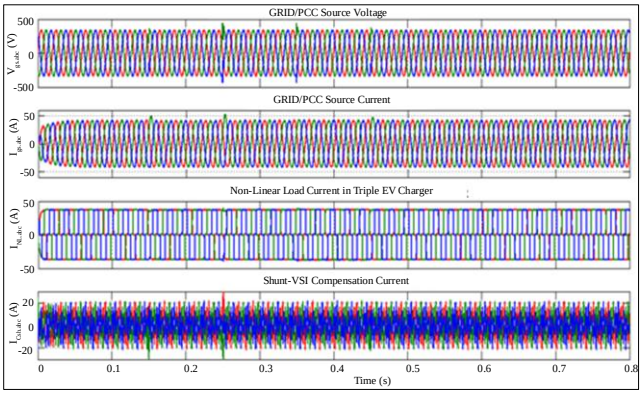

(a) Utility grid/PCC source voltage, (b) Grid/PCC source current, (c) Non-linear load current in triple EV chargers, and (d) Shunt VSI-2 compensation current

Fig. 14 Simulation results of harmonic current compensation in utility-grid/PCC powered triple EV-chargers by using proposed GVCR controlled shunt VSI-2 of MF-AUPQC device

The simulation results of harmonic current compensation in utility-grid/PCC powered triple EV-chargers by using the proposed GVCR controlled shunt VSI-2 of MF-AUPQC device are depicted in Figure 14. The triple-EV chargers comprise three individual non-linear DBRs is employed which are powered by a three-phase distribution network via a utility-grid source with a voltage of $V_{gs.abc}$-415V_{rms} and constant system frequency of F_{gs}-50Hz as shown in Figure 14 (a). The front-end non-linear triple DBR modules in the charging unit are used for charging the EV batteries through the AC to DC conversion principle. During this conversion principle, the triple DBRs inject massive harmful harmonic currents into the PCC of utility-grid system. These massive harmonic currents prompt the distortions in utility-grid/PCC source current grid frequency as they are causing unbalanced loads, increasing the reactive-power demand, non-unity power factor and so on.

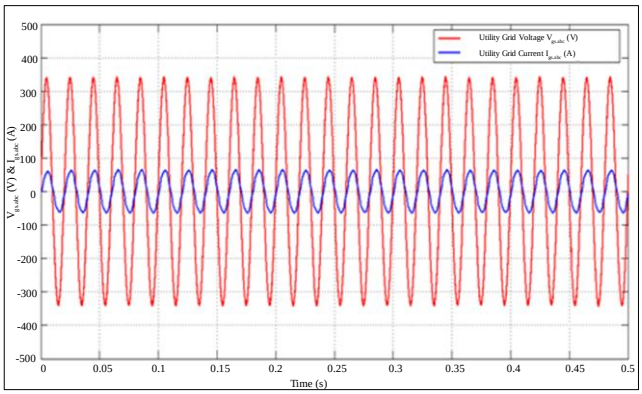

Fig. 15 In-phase of utility-grid/PCC source voltage & current (triple EV chargers)

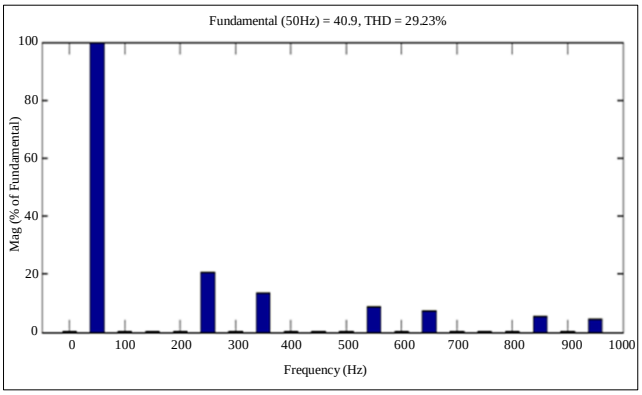

(a) THD spectrum of non-linear load current in triple EV chargers

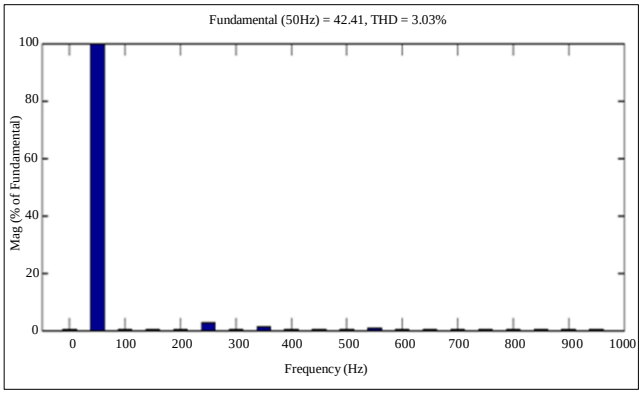

(b) THD spectrum of utility-grid/PCC source current

Fig. 16 THD spectrum analysis during current harmonics compensation (triple EV chargers)

These triple DBR modules are highly influencing the performance and operation of multiple EV charging infrastructures in both communities due to power pollution happening in the PCC of utility-grid systems. For mitigating these issues, the proposed GVCR controlled shunt VSI-2 of

MF-AUPQC device has been enabled for mitigation of massive harmonic current distortions at PCC of utility-grid system.

It functions based on the "in-phase opposition current injection principle", which injects the required compensation current into grid/PCC to make the source current a balanced, linear, sinusoidal and fundamental nature. It maintains the utility-grid/PCC current as a balanced and sinusoidal shape with a value of 42A for delivering the non-linear DBR load current of 37A, as shown in Figures 14(b) and 14(c).

The shunt VSI-2 injects the requisite compensation current of 21A via line interface filters, as shown in Figure 14(d), respectively. Mainly, the proposed GVCR algorithm enables the extraction of fundamental reference currents and helps to produce the feasible switching states to shunt VSI-2 of MF-AUPQC device for PQ enhancement as per IEC/IEEE standards. For this compensation, thus utility-grid/PCC current is served as in-phase with the PCC source voltage to maintain the ideal power factor at the grid/PCC of the distribution network, as shown in Figure 15.

The THD spectrum analysis of the non-linear load current of triple-EV chargers integration is computed with a value of 29.23%. The THD spectrum analysis of utility-grid/PCC source current is computed with a value of 3.03% is depicted in Figures 16(a) and 16(b), which is well-being as per IEEE-519/2022 limits.

4.4. Compensation of Voltage Associated PQ Issues in Utility-Grid/PCC Powered EV-Chargers by Using Proposed GVCR Controlled Shunt VSI-1 of MF-AUPQC Device

The simulation results of voltage associated PQ compensation in utility-grid/PCC-powered EV chargers by using the proposed GVCR controlled series VSI-1 of MF-AUPQC device are shown in Figure 17. The EV chargers comprised of individual non-linear DBR are employed, which is powered by a three-phase distribution network via a utility-grid source with a voltage of Vgs.abc-415Vrms and constant system frequency of Fgs-50Hz as shown in Figure 17(a).

The front-end non-linear DBR modules in the charging unit are used for charging the EV batteries through the AC to DC conversion principle. In this case, the voltage harmonics voltage sags/swells occur in the utility-grid/PCC of the distribution network; these voltage PQ issues disrupt the continuous power flow to EV charging stations. Due to these voltage interruptions, these DBRs are not functioning properly for charging the EV batteries in charging stations.

In this regard, the series-connected VSI-1 of the MF-AUPQC device is considered a series-active power filter for compensation of voltage affected PQ issues such as voltage harmonics, voltage sags-swells, and voltage interruptions occurring in utility-grid/PCC level. When any voltage deviations occur in the utility-grid affecting the grid-code limits, the attained voltage issues are counteracted by series VSI-1 of the MF-AUPQC device.

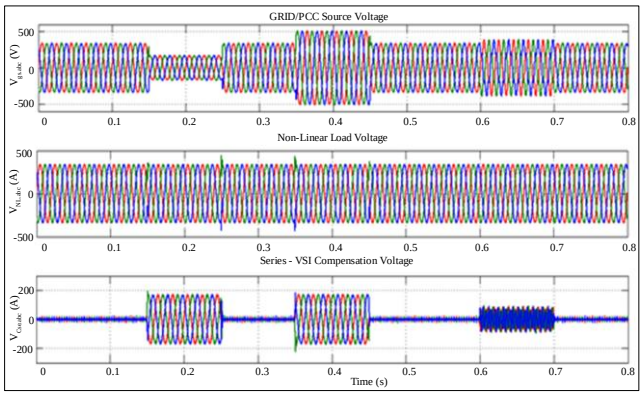

(a) Utility grid/PCC source voltage, (b) Non-linear DBR load voltage, and (c) Series VSI-1 compensation voltage

Fig. 17 Simulation results of voltage associated PQ compensation in utility-grid/PCC powered EV-chargers by using proposed GVCR controlled shunt VSI-1 of MF-AUPQC device

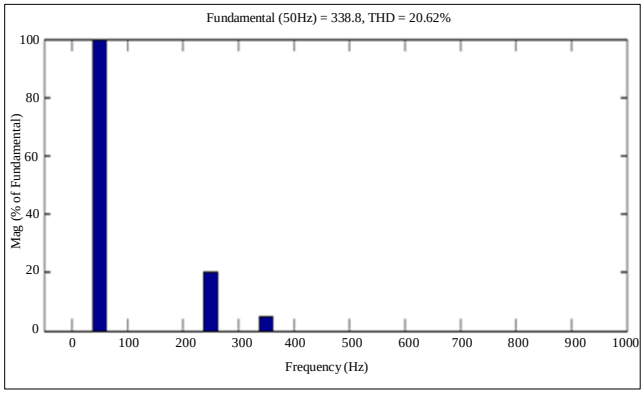

(a) THD spectrum of utility-grid/PCC source voltage

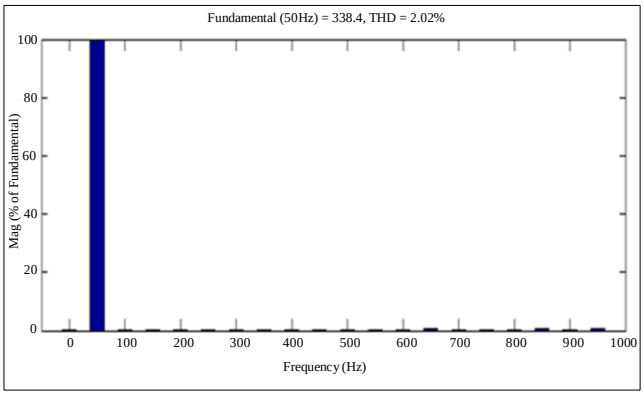

(b) THD spectrum of non-linear DBR load voltage

Fig. 18 Harmonic spectrum analysis during voltage harmonic compensation

This series VSI-1 functions as an "in-phase injection principle", which injects the required voltage into PCC to make non-linear load voltage sinusoidal, balanced, constant and fundamental.

Mainly, the proposed GVCR algorithm enables the extraction of fundamental reference voltages and helps to produce the feasible switching states to series VSI-1 of MF-AUPQC device for PQ enhancement as per IEC/IEEE standards. Before the time period, t_p<0.15 sec is considered a pre-sag state; in this state, utility-grid/PCC voltage is maintained as a constant potential value of 340V.

The voltage-sag has been developed in this time period (0.15 sec<t<0.25 sec), then the utility-grid/PCC voltage is decreased by 50%, which is calculated as 170V and affecting the non-linear DBR load voltage as inconstant. In this period, the series VSI-1 of the MF-AUPQC device injects the required compensation voltage of 170V to maintain the load voltage constant of 340V.

Similarly, the voltage-swell has been developed in this time period (0.35 sec<t<0.45 sec), then the utility-grid/PCC voltage is increased by 50%, which is calculated as 510V and misoperations of non-linear DBR load voltage as inconstant. In this period, the series VSI-1 of the MF-AUPQC device extracts the additional compensation voltage of 170V to maintain the load voltage constant of 340V.

However, the voltage-harmonics has been developed in this time period (0.6 sec<t<0.7 sec), then the utility-grid/PCC voltage is affected as non-sinusoidal and fundamental nature. In this period, the series VSI-1 of MF-AUPQC device injects the compensation voltage as in-phase opposition compensation principle to maintain non-linear DBR load voltage is balanced, sinusoidal shape and fundamental nature as per IEEE standards as shown in Figures 17 (a) to (c).

The THD spectrum analysis of utility-grid/PCC voltage is computed with a value of 20.62%, and the THD spectrum analysis of non-linear DBR voltage is computed with a value of 2.02% is depicted in Figures 18 (a) and 18(b), which is well-being as per IEEE-519/2022 limits.

Table 2. THD comparisons of non-linear DBR load current and utility-grid/PCC current under integration of various EV chargers

Current THD (%)	Classical IRP Controlled MF-AUPQC Device [29]		Proposed GVCR Controlled MF-AUPQC Device	
	Non-Linear DBR Load Current	Utility-Grid/PCC Current	Non-Linear DBR Load Current	Utility-Grid/PCC Current
Integration of Single-EV Charger	30.08%	2.87%	30.18%	1.64%
Integration of Dual-EV Chargers	29.60%	3.91%	29.87%	2.12%
Integration of Triple-EV Chargers	28.05%	6.05%	29.23%	3.03%

Table 3. THD comparisons of utility-grid/PCC voltage & non-linear DBR load voltage under integration of various EV chargers

Voltage THD (%)	Classical SRF Controlled MF-AUPQC Device [30]		Proposed GVCR Controlled MF-AUPQC Device	
	Utility-Grid/PCC Voltage	Non-Linear DBR Load Voltage	Utility-Grid/PCC Voltage	Non-Linear DBR Load Voltage
Integration of Single-EV Charger	20.62%	2.76%	20.62%	1.01%
Integration of Dual-EV Chargers	20.62%	3.29%	20.62%	1.56%
Integration of Triple-EV Chargers	20.62%	4.82%	20.62%	2.02%

The THD comparisons and graphical view of non-linear DBR load current and utility-grid/PCC current under the integration of various EV chargers are illustrated in Table 2 and Figure 19. It is noted that the proposed GVCR control scheme provides the feasible compensation current for the mitigation of harmonic current distortions and also maintains a good harmonic profile compared to the classical IRP control scheme.

The THD comparisons and graphical view of utility-grid/PCC voltage and non-linear DBR load voltage under the integration of various EV chargers are illustrated in Table 3 and Figure 20. It is noted that the proposed GVCR control scheme provides the feasible compensation voltage for the mitigation of voltage harmonics and also maintains a good harmonic profile compared to the classical SRF control scheme.

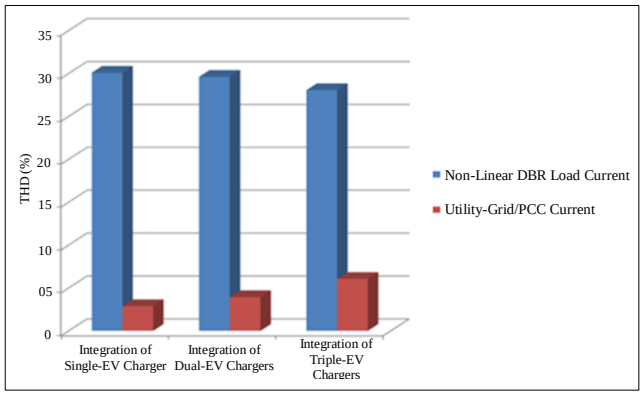

(a) In classical IRP control scheme

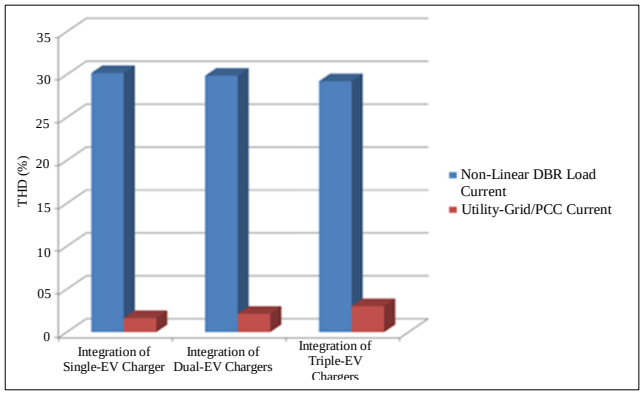

(b) In the proposed GVCR control scheme

Fig. 19 Graphical view of non-linear DBR load current and utility-grid/PCC current under integration of various EV chargers

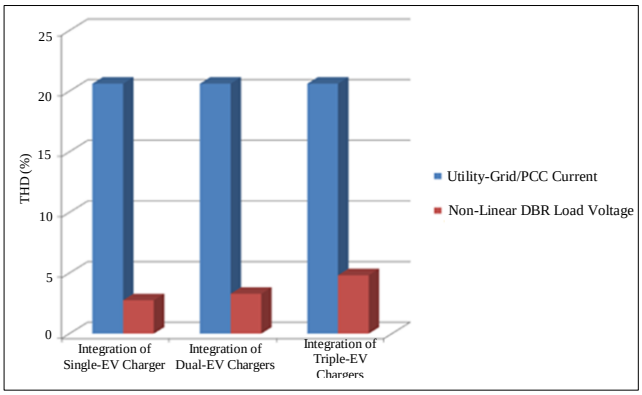

(a) In Classical SRF control scheme

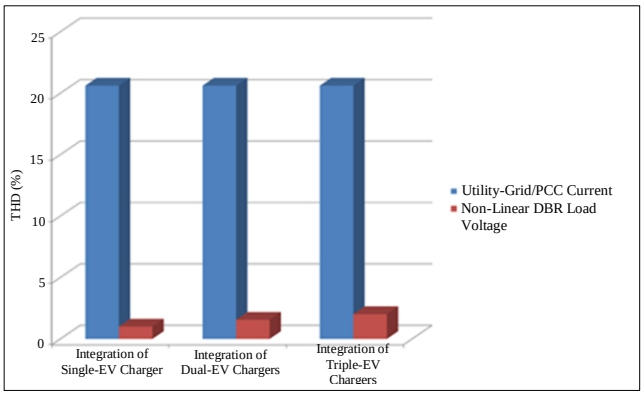

(b) In the proposed GVCR control scheme

Fig. 20 Graphical view of utility-grid/PCC voltage & non-linear DBR load voltage under integration of various EV chargers

4.5. Transition of Utility-Grid to Solar-PV Feeding DG Integrated Utility-Grid/PCC Powered EV-Chargers by Using Proposed GVCR Controlled DG-VSI-1 of MF-AUPQC Device

The simulation results of DG-integrated utility-grid/PCC-powered EV chargers by using proposed GVCR controlled DG-VSI-1 of MF-AUPQC device under transition of utility-grid to solar-PV system is depicted in Figure 21. In general, these EV chargers are energized by three-phase utility-grid/PCC of distribution network with a voltage of $V_{gs.abc}$-$415V_{rms}$ and constant system frequency of F_{gs}-50Hz is shown in Figure 21 (a).

In this case, the operation and performance of the proposed GVCR controlled MF-AUPQC device have been investigated under both DG and PQ mitigation modes under the transition of utility-grid to solar-PV system. In DG mode, the combination of utility-grid and solar-PV power has been used for energizing the EV batteries. During the time instant 0sec<t<0.9sec, the power coming from utility-grid has been used for energizing the EV batteries in the charging station. The VSI-2 of the MF-AUPQC device has functioned as shunt connected active-power filter for compensation of all current affected PQ issues (without DG under solar-irradiance level at S-0 W/m^2).

During time instant 0.9sec<t<1.35sec, the solar-PV is the major source of DG for energizing the EV batteries in the charging station. Moreover, the produced solar-PV power has been controlled by using a front-end DC-DC boost converter with an Incremental-Conductance (INC) Maximum-Power Point Tracker (MPPT) algorithm. The VSI-2 of the MF-AUPQC device has functioned as DG-VSI, which delivers the active power to non-linear DBRs of EV chargers based on the availability of solar PV power.

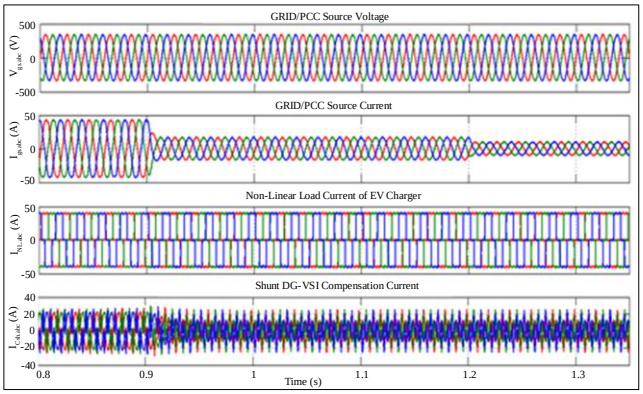

(a)-(d)

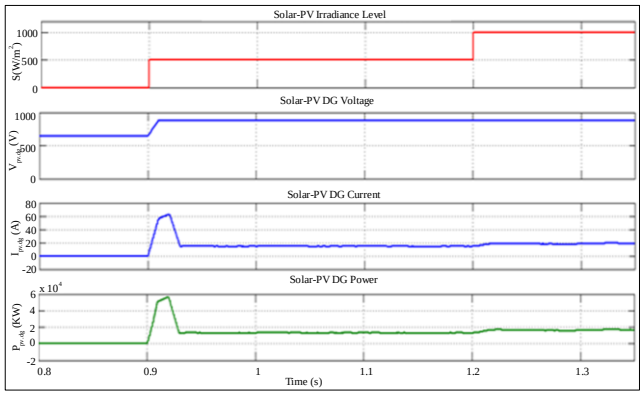

(e)-(h)

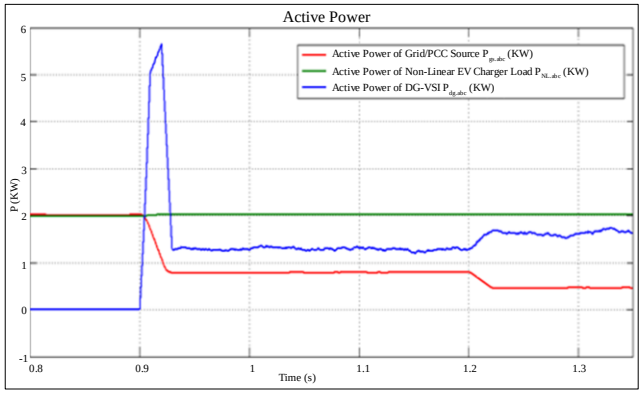

(i)

(a) Utility-grid/PCC voltage, (b) Utility-grid/PCC current, (c) Non-linear DBR load current of EV charger, (d) Shunt DG-VSI-2 compensation current, (e) Solar-PV irradiance, (f) Solar-PV DG Voltage, (g) Solar-PV DG current, (h) Solar-PV power, and (i) Active powers of utility-grid/PCC, non-linear DBR load and VSI-2 injected power in DG integration scheme.

Fig. 21 Simulation results of DG integrated utility-grid/PCC powered EV chargers by using proposed GVCR CONTROLLED DG-VSI-1 of MF-AUPQC device under transition of utility-grid to solar-PV system

The main advantage of the DG scheme is, that it avoids the use of additional complex DG-VSI's and its control droop control algorithm. The shunt DG-VSI-2 of MF-AUPQC device acts as DG-VSI, which saves size, cost and compact energy generation scheme.

During the time instant of 0.9 sec<t<1.2 sec, 50% of solar-PV irradiance level (S-500W/m^2) is available, which means DG has been enabled, the extracted solar-PV power from INC-MPPT algorithm with utility-grid power delivered to EV charging stations. The required non-linear DBR's load current of EV chargers is measured as 42A, which is shared by both utility-grid/PCC current of 17A, and the remaining 25A has been delivered by the solar-PV manifested DG current as current sharing principle as shown in Figure 21 (b) to (d).

During the 50% of solar-PV irradiance level (S-500W/m^2), it extracts the maximum solar-PV voltage of 880V, which is the same as common DC-link voltage with a maximum PV current of 14.7A and the maximum solar-PV power of 13KW is depicted in Figure 21 (e) to (h). Similarly, in this low irradiance level, the DG delivers the minimum active power of 13KW, and the utility-grid system has shared the remaining active power of 7KW to achieve the requisite non-linear DBR load power of 20KW as depicted in Figure 21 (i).

During the time instant of 1.2 sec<t<1.35 sec, 100% of solar-PV irradiance level (S-1000W/m^2) is available, which means DG has been enabled, the extracted solar-PV power from INC-MPPT algorithm with utility-grid power delivered to EV charging stations. The required non-linear DBR's load current of EV chargers is measured as 42A, which is shared by both utility-grid/PCC current of 10A, and the remaining 32A has been delivered by the solar-PV manifested DG current as current sharing principle as shown in Figure 21 (b) to (d).

During the 100% of solar-PV irradiance level (S-1000W/m^2), it extracts the maximum solar-PV voltage of 880V, which is the same as the common DC-link voltage with a maximum PV current of 19.3A and the maximum solar-PV power of 17KW is depicted in Figure 21 (e) to (h). Similarly, in this high irradiance level, the DG delivers the maximum active power of 17KW, and the utility-grid system has shared the remaining active power of 3KW to achieve the requisite non-linear DBR load power of 20KW as depicted in Figure 21 (i).

4.6. Transition of Solar-PV to Utility-Grid Feeding DG Integrated Utility-Grid/PCC Powered EV-Chargers by Using Proposed GVCR Controlled DG-VSI-1 of MF-AUPQC Device

The simulation results of DG integrated utility-grid/PCC powered EV chargers by using proposed GVCR controlled DG-VSI-1 of MF-AUPQC device under transition of solar-PV to utility-grid system is depicted in Figure 22. In general, these EV chargers are energized by three-phase utility-grid/PCC of distribution network with a voltage of $V_{gs.abc}$-415V_{rms} and constant system frequency of F_{gs}-50Hz is shown in Figure 22 (a).

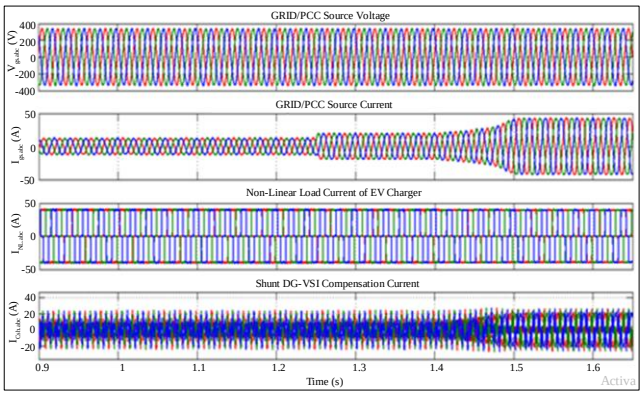

(a)-(d)

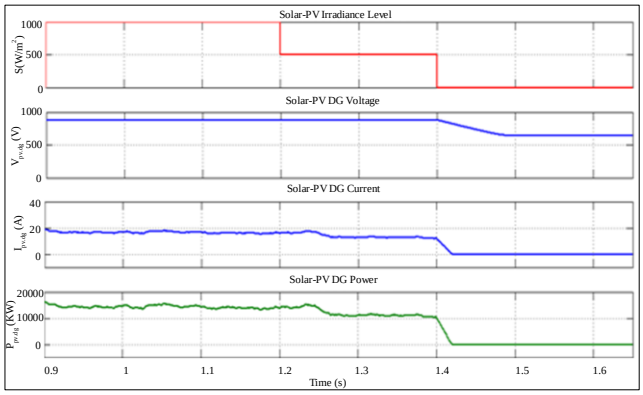

(e)-(h)

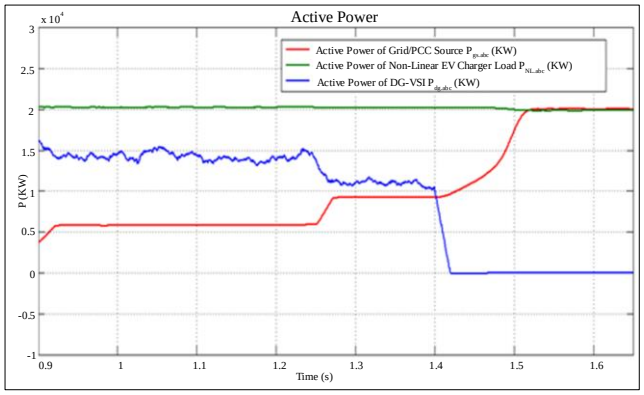

(i)

(a) Utility-grid/PCC voltage, (b) Utility-grid/PCC current, (c) Non-linear DBR load current of EV charger, (d) Shunt DG-VSI-2 compensation current, (e) Solar-PV irradiance, (f) Solar-PV DG voltage, (g) Solar-PV DG current, (h) Solar-PV power, and (i) Active powers of utility-grid/PCC, non-linear DBR load and VSI-2 injected power in DG integration scheme

Fig. 22 Simulation results of DG integrated utility-grid/PCC powered EV chargers by using proposed GVCR controlled DG-VSI-1 of MF-AUPQC device under transition of solar-PV to utility-grid system

In this case, the operation and performance of the proposed GVCR controlled MF-AUPQC device have been investigated under both DG and PQ mitigation modes under the transition of solar-PV to utility-grid system. In DG mode, the combination of solar-PV and utility-grid power has been used for energizing the EV batteries.

During time instant 0.9sec<t<1.4sec, the solar-PV is the major source of DG for energizing the EV batteries in the charging station. The produced solar-PV power has been controlled by using a front-end DC-DC boost converter with an Incremental-Conductance (INC) Maximum-Power Point Tracker (MPPT) algorithm. The VSI-2 of the MF-AUPQC device has functioned as DG-VSI, which delivers the active power to non-linear DBRs of EV chargers based on the availability of solar PV power. The main advantage of the DG scheme is, that it avoids the use of additional complex DG-VSI's and its control droop control algorithm. The shunt DG-VSI-2 of MF-AUPQC device acts as DG-VSI, which saves size, cost and compact energy generation scheme. During the time instant of 0.9 sec<t<1.25 sec, 100% of solar-PV irradiance level (S-1000W/m^2) is available, which means DG has been enabled fully, the extracted solar-PV power from INC-MPPT algorithm with utility-grid power delivered to EV charging stations. The required non-linear DBR's load current of EV chargers is measured as 42A, which is shared by both utility-grid/PCC current of 8A, and the solar-PV has delivered the remaining 34A manifested DG current as current sharing principle as shown in Figure 22 (b) to (d).

During the 100% of solar-PV irradiance level (S-1000W/m^2), it extracts the maximum solar-PV voltage of 880V, which is the same as the common DC-link voltage with a maximum PV current of 17.05A and the maximum solar-PV power of 14.5KW is depicted in Figure 22 (e) to (h). Similarly, in this high irradiance level, the DG delivers the maximum active power of 14.5KW, and the utility-grid system has shared the remaining active power of 5.5KW to achieve the requisite non-linear DBR load power of 20KW as depicted in Figure 22 (i).

During the time instant of 1.25 sec<t<1.4 sec, 50% of solar-PV irradiance level (S-500W/m^2) is available, which means DG has been enabled, the extracted solar-PV power from INC-MPPT algorithm with utility-grid power delivered to EV charging stations. The required non-linear DBR's load current of EV chargers is measured as 42A, which is shared by both utility-grid/PCC current of 20A, and the solar-PV has delivered the remaining 22A manifested DG current as current sharing principle as shown in Figure 22 (b) to (d).

During the 50% of solar-PV irradiance level (S-500W/m^2), it extracts the minimum solar-PV voltage of 880V, which is the same as common DC-link voltage with a minimum PV current of 12.5A and the maximum solar-PV power of 10.8KW is depicted in Figure 22 (e) to (h). Similarly, in this low irradiance level, the DG delivers the minimum active power of 10.8KW, and the utility-grid system has shared the remaining active power of 9.2KW to achieve the requisite non-linear DBR load power of 20KW as depicted in Figure 22 (i).

During the time instant 1.4sec<t<1.65sec, the power coming from utility-grid has been used for energizing the EV batteries in the charging station. The VSI-2 of the MF-AUPQC device has been functioning as a shunt shunt-connected active-power filter for compensation of all current affected PQ issues (without DG under solar-irradiance level is at S-0 W/m^2). The comparison of active powers of the utility-grid, DG-VSI-2 injected power, and non-linear DBR load power under transition of utility-grid to solar-PV integrated DG scheme is illustrated in Table 4. The comparison of active powers of utility-grid, DG-VSI-2 injected power and non-linear DBR load power under transition of solar-PV to utility-grid integrated scheme is illustrated in Table 5.

Table 4. Comparison of active powers of utility-grid, DG-VSI-2 injected power and non-linear DBR load power under transition of utility-grid to solar-PV integrated DG scheme

Time Instants	Utility-Grid Power	DG-VSI-2 Injected Power	Non-Linear DBR Load Power
0sec<t<0.9sec	20KW	0KW	20KW
0.9sec<t<1.2sec	7KW	13KW	20KW
1.2sec<t<1.35sec	3KW	17KW	20KW

Table 5. Comparison of active powers of utility-grid, DG-VSI-2 injected power and non-linear DBR load power under transition of solar-PV to utility-grid integrated scheme

Time Instants	Utility-Grid Power	DG-VSI-2 Injected Power	Non-Linear DBR Load Power
0.9sec<t<1.25sec	5.5KW	14.5KW	20KW
1.25sec<t<1.4sec	9.2KW	10.8KW	20KW
1.4sec<t<1.65sec	20KW	0KW	20KW

5. Conclusion

In this work, a novel GVCR controlled MF-AUPQC device has been proposed for the effective performance of PQ enhancement and DG integration in utility-grid powered EV charging stations. The proposed MF-AUPQC device acts as a multi-functional compensation device. It optimizes both the voltage and current affected PQ issues in both the utility grid and the charging station levels. The proposed GVCR controller enables the extraction of the fundamental reference frequency and helps to generate the feasible switching pattern to both VSI-1 2, which improves voltage and current harmonic profile compared to classical SRF/IRP control algorithms. The key merits are simple mathematical notations, no transformations, fast response, low dv/dt switch stress, low switching loss and maximum efficiency. Moreover, the usage of utility-grid power has been reduced during the DG integration scheme, and the solar PV system has delivered the maximum active power requirement of non-linear DBR load with respect to load demand. The proposed DG scheme avoids the use of additional complex DG-VSI's and its control droop control algorithms for exchanging the active power during scheduled block-outs, sudden load interruptions, power shortages, and grid-islanding problems. The operation and performance of the proposed GVCR controlled MF-AUPQC device are investigated under both DG and PQ mitigation modes by using the Matlab/Simulink computing tool. The simulation results are well-being, complying with IEEE-519/2022 limits.

References

[1] Iqbal Husain et al., "Electric Drive Technology Trends, Challenges, and Opportunities for Future Electric Vehicles," *Proceedings of the IEEE*, vol. 109, no. 6, pp. 1039-1059, 2021. [CrossRef] [Google Scholar] [Publisher Link]

[2] Bo Maclnnis, and Jon A. Krosnick, Climate Insights 2020: Electric Vehicles, Resources for the Future (RFF), 2020. [Online]. Available: https://www.rff.org/publications/reports/climateinsights2020-electric-vehicles.

[3] J.C. Gomez, and M.M. Morcos, "Impact of EV Battery Chargers on the Power Quality of Distribution Systems," *IEEE Transactions on Power Delivery*, vol. 18, no. 3, pp. 975-981, 2003. [CrossRef] [Google Scholar] [Publisher Link]

[4] Kevin J. Dyke, Nigel Schofield, and Mike Barnes, "The Impact of Transport Electrification on Electrical Networks," *IEEE Transactions on Industrial Electronics*, vol. 57, no. 12, pp. 3917-3926, 2010. [CrossRef] [Google Scholar] [Publisher Link]

[5] G. Papaefthymiou et al., "Distributed Generation vs Bulk Power Transmission," *2008 First International Conference on Infrastructure Systems and Services: Building Networks for a Brighter Future (INFRA)*, Netherlands, pp. 1-6, 2008. [CrossRef] [Google Scholar] [Publisher Link]

[6] Tianqiao Zhao et al., "A Flexible Operation of Distributed Generation in Distribution Networks with Dynamic Boundaries," *IEEE Transactions on Power Systems*, vol. 35, no. 5, pp. 4127-4130, 2020. [CrossRef] [Google Scholar] [Publisher Link]

[7] Mohammad Al-Muhaini, and Gerald T. Heydt, "Evaluating Future Power Distribution System Reliability Including Distributed Generation," *IEEE Transactions on Power Delivery*, vol. 28, no. 4, pp. 2264-2272, 2013. [CrossRef] [Google Scholar] [Publisher Link]

[8] J.M. Rondina, L. Martins Neto, and M.B. Alves, "Technology Alternative for Enabling Distributed Generation," *IEEE Latin America Transactions*, vol. 14, no. 9, pp. 4089-4096, 2016. [CrossRef] [Google Scholar] [Publisher Link]

[9] Fei Liu et al., "Utilizing Aggregated Distributed Renewable Energy Sources with Control Coordination for Resilient Distribution System Restoration," *IEEE Transactions on Sustainable Energy*, vol. 14, no. 2, pp. 1043-1056, 2023. [CrossRef] [Google Scholar] [Publisher Link]

[10] Abdulraheem H. Alobaidi et al., "Distribution Service Restoration with Renewable Energy Sources: A Review," *IEEE Transactions on Sustainable Energy*, vol. 14, no. 2, pp. 1151-1168, 2023. [CrossRef] [Google Scholar] [Publisher Link]

[11] Amresh Kumar Singh, Shailendra Kumar, and Bhim Singh, "Solar PV Energy Generation System Interfaced to Three Phase Grid with Improved Power Quality," *IEEE Transactions on Industrial Electronics*, vol. 67, no. 5, pp. 3798-3808, 2020. [CrossRef] [Google Scholar] [Publisher Link]

[12] Shailendra Kumar, and Bhim Singh, "A Multipurpose PV System Integrated to a Three-Phase Distribution System Using an LWDF-Based Approach," *IEEE Transactions on Power Electronics*, vol. 33, no. 1, pp. 739-748, 2018. [CrossRef] [Google Scholar] [Publisher Link]

[13] S.J. Steffel et al., "Integrating Solar Generation on the Electric Distribution Grid," *IEEE Transactions on Smart Grid*, vol. 3, no. 2, pp. 878-886, 2012. [CrossRef] [Google Scholar] [Publisher Link]

[14] Surbhi Pankaj et al., "Electric Vehicle Charging Stations and their Impact on the Power Quality of Utility Grid," *2022 International Conference on Decision Aid Sciences and Applications (DASA)*, Thailand, pp. 816-821, 2022. [CrossRef] [Google Scholar] [Publisher Link]

[15] Xiao-Ping Zhang, and Zuanhong Yan, "Energy Quality: A Definition," *IEEE Open Access Journal of Power and Energy*, vol. 7, pp. 430-440, 2020. [CrossRef] [Google Scholar] [Publisher Link]

[16] Omar N. Nezamuddin, Clayton L. Nicholas, and Euzeli Cipriano Dos Santos, "The Problem of Electric Vehicle Charging: State-of-the-Art and an Innovative Solution," *IEEE Transactions on Intelligent Transportation Systems*, vol. 23, no. 5, pp. 4663-4673, 2022. [CrossRef] [Google Scholar] [Publisher Link]

[17] Suneet Singh, and Shimi Sudha Letha, "Various Custom Power Devices for Power Quality Improvement: A Review," *2018 International Conference on Power Energy, Environment and Intelligent Control (PEEIC)*, India, pp. 689-695, 2018. [CrossRef] [Google Scholar] [Publisher Link]

[18] Yahia M. Esmail et al., "Mitigating Power Quality Disturbances in Smart Grid Using FACTS," *Indonesian Journal of Electrical Engineering and Computer Science (IJEECS)*, vol. 22, no. 3, pp. 1223-1235, 2021. [CrossRef] [Google Scholar] [Publisher Link]

[19] Eklas Hossain et al., "Analysis and Mitigation of Power Quality Issues in Distributed Generation Systems Using Custom Power Devices," *IEEE Access*, vol. 6, pp. 16816-16833, 2018. [CrossRef] [Google Scholar] [Publisher Link]

[20] Javier Roldán-Pérez et al., "On the Power Flow Limits and Control in Series-Connected Custom Power Devices," *IEEE Transactions on Power Electronics*, vol. 31, no. 10, pp. 7328-7338, 2016. [CrossRef] [Google Scholar] [Publisher Link]

[21] Tejinder Singh Saggu, and Lakhwinder Singh, "Comparative Analysis of Custom Power Devices for Power Quality Improvement in Non-Linear Loads," *2015 2nd International Conference on Recent Advances in Engineering & Computational Sciences (RAECS)*, India, pp. 1-5, 2015. [CrossRef] [Google Scholar] [Publisher Link]

[22] N. Gowtham, and Shobha Shankar, "UPQC: A Custom Power Device for Power Quality Improvement", *Materials Today: Proceedings*, vol. 5, no. 1, pp. 965-972, 2018. [CrossRef] [Google Scholar] [Publisher Link]

[23] G. Satyanarayana et al., "A Critical Evaluation of Power Quality Features Using Hybrid Multi-Filter Conditioner Topology," *Green Computing Communication and Conservation of Energy (ICGCE) 2013 International Conference*, pp. 731-736, 2013. [CrossRef] [Google Scholar] [Publisher Link]

[24] G. Satyanarayana, and K. Lakshmi Ganesh, "Tuning a Robust Performance of Adaptive Fuzzy-PI Driven DSTATCOM for Non-Linear Process Applications," *Springer LNCS Series*, pp. 523-533, 2015. [CrossRef] [Google Scholar] [Publisher Link]

[25] Naeem Abas et al., "Power Quality Improvement Using Dynamic Voltage Restorer," *IEEE Access*, vol. 8, pp. 164325-164339, 2020. [CrossRef] [Google Scholar] [Publisher Link]

[26] Yonghui Ling, Yanjun Li, and Ji Xiang, "Load Support by Droop-Controlled Distributed Generations," *IEEE Transactions on Industrial Electronics*, vol. 68, no. 9, pp. 8345-8355, 2021. [CrossRef] [Google Scholar] [Publisher Link]

[27] Jiancheng Zhang, Bo Sun, and Daduan Zhao, "A Novel Event-Triggered Secondary Control Strategy for Distributed Generalized Droop Control in Microgrid Considering Time Delay," *IEEE Transactions on Power Electronics*, vol. 38, no. 5, pp. 5963-5978, 2023. [CrossRef] [Google Scholar] [Publisher Link]

[28] Nikita Hari, K. Vijayakumar, and Subhranshu Sekhar Dash, "A Versatile Control Scheme for UPQC for Power Quality Improvement," *2011 International Conference on Emerging Trends in Electrical and Computer Technology*, India, pp. 453-458, 2011. [CrossRef] [Google Scholar] [Publisher Link]

[29] K. Palanisamy et al., "Instantaneous Power Theory Based Unified Power Quality Conditioner (UPQC)," *2010 Joint International Conference on Power Electronics, Drives and Energy Systems & 2010 Power India*, India, pp. 1-5, 2010. [CrossRef] [Google Scholar] [Publisher Link]

[30] Metin Kesler, and Engin Ozdemir, "Synchronous-Reference-Frame-Based Control Method for UPQC Under Unbalanced and Distorted Load Conditions," *IEEE Transactions on Industrial Electronics*, vol. 58, no. 9, pp. 3967-3975, 2011. [CrossRef] [Google Scholar] [Publisher Link]